



Optimized sequential extraction for carbonates: Quantification and $\delta^{13}\text{C}$ analysis of calcite, dolomite and siderite



Alejandra Morera-Chavarría^{a,*}, Jasper Griffioen^{b,c}, Thilo Behrends^a

^a Faculty of Geosciences, Department of Earth Sciences, Utrecht University, P.O. Box 80 021, 3508 TA Utrecht, The Netherlands

^b Copernicus Institute of Sustainable Development, Utrecht University, P.O. Box 80 115, 3508 TC Utrecht, The Netherlands

^c TNO Geological Survey of the Netherlands, P.O. Box 80 015, 3508 TA Utrecht, The Netherlands

ARTICLE INFO

Article history:

Received 30 May 2016

Received in revised form 16 September 2016

Accepted 19 September 2016

Available online 20 September 2016

Keywords:

Siderite

Calcite

Dolomite

Acid digestion

Sequential extraction

$\delta^{13}\text{C}$

Sediments

Iron biogeochemistry

ABSTRACT

Siderite is present in diverse types of rocks and sediments, but its quantification is cumbersome when present in relatively low contents. A new analytical method for the sequential separation of different carbonate phases is presented. The separation, quantification and characterization of the carbonates is based on different kinetic reactions during acid digestion in combination with monitoring the solution composition and the concomitant release of CO_2 . Trapping the released gasses permits the isotopic characterization ($\delta^{13}\text{C}$) of the different phases. Based on published rate laws, an idealized model was built to identify pH and temperature conditions for optimal separation of the various carbonates by taking the size distribution of carbonate particles into consideration. Results from the theoretical survey were implemented in an extraction scheme, which was optimized and evaluated by tests on pure mineral phases and their mixtures. Further tests on a diverse array of sediment and rock samples validated the specificity and reproducibility of the method.

© 2016 Elsevier B.V. All rights reserved.

1. Introduction

Siderite (FeCO_3) is a common diagenetic iron-bearing mineral. It has been reported in a variety of depositional systems, ranging from terrestrial to marine environments (Curtis et al., 1975; Postma, 1981; Postma, 1982; Mozley, 1989; Mozley & Wersin, 1992; Haese et al., 1997; Amirbahman et al., 1998; Hartog et al., 2002). Siderite is present in sediment layers in disseminated form and as concretions (Pearson, 1974; Mozley & Carothers, 1992; Haese et al., 1997; Mortimer et al., 2011). Traditionally, the occurrence and geochemical properties of siderite in sediments are used as important indicators for diagenetic processes, preservation of the sedimentary records and pore water chemistry (Curtis et al., 1975; Gautier, 1982; Mozley & Wersin, 1992; Albani et al., 2001). The isotopic signatures ($\delta^{13}\text{C}$, $\delta^{18}\text{O}$) present in concretions are used for the determination of depositional environments and formation conditions (Matsumoto, 1989; Mozley & Carothers, 1992; Mortimer and Coleman, 1997; Fisher et al., 1998; Wilkinson et al., 2000; Albani et al., 2001; Sapota et al., 2006; Huggett et al., 2010). Also, carbonate clumped isotopes analysis of siderite has been used as paleoclimate proxy for humid continental environments (Fernandez et al., 2014).

The $\delta^{13}\text{C}$ of carbonates can be used to identify the major source for inorganic carbon in rocks and sediments (Curtis et al., 1986). The various sources for inorganic carbon typically exhibit large differences in $\delta^{13}\text{C}$. The value for $\delta^{13}\text{C}$ of atmospheric CO_2 is $\sim -7\text{‰}$ (Craig, 1953; Meyers, 1994). In sediments, respiration of organic matter (OM) is commonly the major source for inorganic carbon of authigenic carbonates. OM has a wide range of $\delta^{13}\text{C}$ values (-32 to -11‰) depending on the carbon fixation pathway (Meyers, 1994) and the carbon isotope signature of OM is used to distinguish marine and terrestrial input (Sackett, 1964). Often, methane oxidation is coupled to the formation of carbonates. Methane is isotopically light with $\delta^{13}\text{C}$ values between -110 and -50‰ (Whiticar, 1999) and in particular carbonates produced by anaerobic methane oxidation are exceptionally depleted in ^{13}C ($\delta^{13}\text{C}$ values between -50 to -125‰) (Baker and Fritz, 1981; Drake et al., 2015). In contrast, carbonates formed during methanogenesis tend to have high $\delta^{13}\text{C}$ values of above 12‰ (Curtis et al., 1986; Budai et al., 2002).

Even in small quantities, siderite has relevant environmental implications. In groundwater systems siderite may act as a source or sink for contaminants such as arsenic (Guo et al., 2007; Jönsson & Sherman, 2008); it also functions as an important controller of iron concentrations and alkalinity (Hartog et al., 2002; Antoniou et al., 2012; Griffioen et al., 2013). Furthermore, siderite has an important role in radioactive waste storage due to its capacity to immobilise radionuclides such as ^{79}Se and ^{238}U (Scheinost and Charlet, 2008; Ithurbide et al.,

* Corresponding author.

E-mail addresses: a.morerachavarría@uu.nl (A. Morera-Chavarría), jasper.griffioen@tno.nl (J. Griffioen), t.behrends@uu.nl (T. Behrends).

2009; Ithurburde et al., 2010). In addition, siderite has been recognized as a key secondary product of CO₂ capture and storage in geological formations (Johnson et al., 2004; Rochelle et al., 2004; Lal, 2008).

In many settings, siderite is closely associated with other carbonates such as calcite, dolomite, rhodochrosite and corresponding solid solutions (Postma, 1977; Postma, 1981; Curtis et al., 1986; Saunders & Swann, 1992; Stemberck & Sohlenius, 1997; Rossi et al., 2001). The separation of siderite from these mineral associations has been described as challenging (Pearson, 1974; Pye et al., 1990; Sitko et al., 2009): the identification, quantification and geochemical characterization of siderite in sediments are complicated. The identification or characterization of carbonate phases has been approached by different methods including spectroscopic techniques (König & Hollatz, 1990; Spadini et al., 2003; Das and Hendry, 2011; Boulard et al., 2012), thermal analysis (Smykatz-Kloss, 1982; Dell'Abate et al., 2003) and XRD (Hill and Howard, 1987; Bish and Post, 1993; Weidler et al., 1998). These methods vary regarding their sensitivity and suitability (Kulp et al., 1951; Warne et al., 1981; König & Hollatz, 1990; Haese et al., 1997; Ward & Gómez-Fernández, 2003; Pecharsky & Zavalij, 2009), but the quantification of low amounts of siderites in carbonate mixtures remains challenging by either of those, and they do not allow isotopic characterization. Sequential extractions bear the potential for characterizing the extraction products regarding their isotopic composition in combination with the quantification of the target phases.

Selective chemical extractions have been widely used to characterize the partitioning of elements between different solids in sediments and soils (Chester & Hughes, 1967; Tessier et al., 1979; Haese et al., 1997). In these extraction schemes, the carbonate-bound elements are processed in a single step, often focusing on calcite and assigning only a secondary role to other carbonate minerals (such as dolomite and siderite). Sequential extractions for the differentiation between iron phases have been developed for sediments and soils including extraction steps targeting carbonate-bound iron (Haese et al., 1997; Poulton & Canfield, 2005; Claff et al., 2010). The selectivity of these extractions has been questioned as reagents used for the dissolution of carbonates in sequential extraction methods may not dissolve completely siderite or dolomite and may enhance dissolution of other Fe-bearing phases as Fe oxyhydroxides, vivianite and Fe sulphides (Tessier et al., 1979; Haese et al., 1997; Vriens, 2011; Egger et al., 2015). The selectivity of each step in a sequential extraction scheme depends on factors such as the grain size distribution of the phases, the intrinsic difference in dissolution kinetics and other factors controlling dissolution kinetics as the surface density of the reactive sites or crystal imperfections (Tessier et al., 1979; Alkattan et al., 1998; Gautelier et al., 1999; Morse & Arvidson, 2002; Pokrovsky et al., 2009; Golubev et al., 2009).

Standard protocols have been established for isotopic analysis of different carbonates. These protocols are based on the method described by McCrea (1950), in which concentrated phosphoric acid is used to dissolve carbonates and the released CO₂ is collected and analysed by mass spectrometry. The kinetic parameters for the dissolution of individual carbonates in phosphoric acid have been determined by McCrea (1950), Clayton et al. (1968), Becker and Clayton (1972) and Rosenbaum & Sheppard (1986). This method has been applied to carbonates mixtures but joined dissolution of the different carbonates in the mixtures and isotopic fractionation upon partial digestion of carbonates have been reported (Degens & Epstein, 1964; Walters et al., 1972; Carothers et al., 1988; Al-Aasam et al., 1990). The advantage of using concentrated phosphoric acid to dissolve carbonates is that determination of both $\delta^{13}\text{C}$ and $\delta^{18}\text{O}$ is possible. However, the possibility to optimize the separation between different carbonates is limited as the corrosivity of the solution cannot be adjusted. Furthermore, it is difficult to evaluate the selectivity of each step by monitoring the solution composition and to use the extraction procedure to simultaneously determining the content of the various carbonates.

If only the least reactive carbonate phase is of interest, another approach can be taken by completely leaching the more reactive phases

and subsequently analysing the remaining most stable phase. For example, Swart & Melim (2000) used repetitive leaching with acetic acid to isolate dolomite in carbonate mixtures and used XRD to monitor the progress of leaching other carbonates. Loss of dolomite is inevitable when following this approach, implying the possibility of fractionation artefacts. Furthermore, this approach does not allow to combine the isotopic characterization of dolomite with its quantification and the characterization of the less reactive phases.

This study aims to develop a new analytical method for the sequential separation of different carbonate phases in sediment samples, specifically focussing on the separation of siderite from other carbonate and iron phases. In order to reduce the ambiguity of sequential extractions and to quantify the various carbonates, the method combines measuring the release of Ca²⁺, Mg²⁺ and Fe²⁺ into solution with determining the concomitant release of CO₂ and H₂S. Capturing the released CO₂ permits the isotopic characterization ($\delta^{13}\text{C}$) of the dissolved carbonates. Natural samples of various carbonates (calcite, dolomite and siderite) were used for the optimization of the experimental conditions controlling the acid dissolution kinetics. These minerals were selected due to their common association in various sedimentary and metamorphic environments (Becker and Clayton, 1972; Huisman et al., 2000; Hartog et al., 2005; Craddock and Dauphas, 2011; Antoniou et al., 2012; Griffioen et al., 2016).

2. Theoretical considerations

Differences in dissolution kinetics determine the specificity of sequential extractions. Rates of mineral dissolution are typically controlled by various factors including pH, temperature, pressure, specific surface area, surface morphological imperfections and the presence of other solutes that can enhance or inhibit mineral dissolution (Stumm & Morgan, 1996; Alkattan et al., 2002). In view of the acidic dissolution of carbonates, the obvious parameters which can be varied to achieve selectivity are pH and temperature. In order to identify suitable conditions for the separation of carbonates we survey the role of pH, temperature, time and grain size on the extent of dissolution of calcite, dolomite and siderite based on reported rate laws.

2.1. Main kinetic parameters

The dissolution kinetics of calcite have been extensively studied under diverse conditions and with emphasis of rate-determining parameters, such as pH (Berner and Morse, 1974; Sjöberg & Rickard, 1984a; Sjöberg & Rickard, 1984b; Van Cappellen et al., 1993; Alkattan et al., 1998), temperature (Plummer et al., 1978; Sjöberg & Rickard, 1984b; Alkattan et al., 1998), P_{CO_2} (Plummer et al., 1978) and ionic strength (Berner and Morse, 1974; Alkattan et al., 2002). In contrast, there have been fewer studies on the dissolution kinetics of dolomite and siderite (Gautelier et al., 1999; Golubev et al., 2009). The reaction rates of the dissolution of carbonates are often controlled and categorized by: 1) the detachment of chemical species from the mineral surface (chemically controlled kinetics) and 2) the diffusive transport of the dissolved aqueous species from this surface through the diffusion boundary layer (DBL) into bulk solution (transport-controlled kinetics) (Rickard & Sjöberg, 1983; Sjöberg & Rickard, 1984a; Alkattan et al., 1998; Gautelier et al., 1999).

According to Pokrovsky et al. (2009) the kinetic rate law for the chemical dissolution of carbonates (Eq. (1)) is based on three chemical reactions (Plummer et al., 1978; Chou et al., 1989; Wollast, 1990) whose relevance for the dissolution rates depend on pH via three parallel pathways: 1) the protonation of the surface (relevant at $\text{pH} \leq 5$), 2) the carbonation of the surface (relevant at $4 \leq \text{pH} \leq 6$) and 3) the reversible attachment and release of metal and carbonate ions (relevant at $\text{pH} > 6$).

$$R = k_1 * \alpha_{\text{H}^+} + k_2 * \alpha_{\text{H}_2\text{CO}_3} + k_3 - k_{-3} * \alpha_{\text{Me}^{2+}} * \alpha_{\text{CO}_3^{2-}} \quad (1)$$

where k_i is the rate constants for reaction i and α is the activity of the aqueous species. At $\text{pH} < 4$, transport has a strong control over the dissolution of calcite (Berner and Morse, 1974; Sjöberg & Rickard, 1984a; Wollast, 1990) and to a lesser extent on dolomite and siderite dissolution (Gautelier et al., 1999; Pokrovsky et al., 2009; Golubev et al., 2009).

An increase in temperature generally leads to an increase in the rate constants and diffusion coefficients (Alkattan et al., 1998). The temperature dependence of carbonate dissolution might also exert influence on the order of the reaction (n) in Eq. (1). For calcite, a value of 1.0 was consistently used at different temperatures (Alkattan et al., 1998; Alkattan et al., 2002). However, for dolomites and siderites, the rates have been reported to change the order with differing temperatures (Lund et al., 1973; Busenberg and Plummer, 1982; Chou et al., 1989; Gautelier et al., 1999; Lüttge et al., 2003; Duckworth & Martin, 2004a; Duckworth & Martin, 2004b; Golubev et al., 2009).

In addition to solution composition and physical conditions, grain size and surface properties are important factors controlling the kinetics of carbonates dissolution. Differences in dissolution rates of a carbonate phase have been attributed to morphological factors such as surface area, distribution of reactive surface sites, grain size and, in the case of biogenic calcites, microstructures (Morse & Arvidson, 2002).

2.2. Critical radius of a carbonate particle for acid dissolution

Siderite is often present in combination with calcite and/or dolomite in rocks and sediments. The pH, time and temperature are parameters, which can be easily tuned for separating these carbonates. To identify the conditions for optimal separation of the various carbonates regarding their dissolution kinetics, we first evaluate the role of these parameters on the evolution of the grain size during the acid dissolution of the respective carbonates. Clayton et al. (1968) and Walters et al. (1972) pointed out that particle size is important regarding the effectiveness of the extraction and the related risk of fractionation during acid dissolution of carbonates. Therefore, we calculated the critical radii, which correspond to nearly complete dissolution ($\geq 95\%$) and insubstantial dissolution ($< 5\%$) of calcite, dolomite and siderite at acidic conditions ($\text{pH} \leq 5$) and temperatures that range between 30 and 100 °C (Table 1). For this, averaged reported rates for calcite (Alkattan et al., 1998; Morse & Arvidson, 2002; Pokrovsky et al., 2009), dolomite (Gautelier et al., 1999; Morse & Arvidson, 2002) and siderite (Golubev et al., 2009) were used. In all studies a batch or mixed-flow reactor coupled to rotating disk technique was used for measuring the reaction rates, with the exception of Morse & Arvidson (2002) who used a compilation of data from different literature sources.

Table 1
Shrinking rate (dr/dt) during acid dissolution of calcite, dolomite and siderite calculated from reported, experimentally derived dissolution rates. Dissolution rates indicated with * are interpolated rates from the listed reference. The dissolution rates correspond to the following references: (1) Alkattan et al. (1998), (2) Pokrovsky et al. (2009), (3) Morse & Arvidson (2002), (4) Gautelier et al. (1999) and (5) Golubev et al. (2009).

Mineral	Temperature (°C)	pH	Stirring (rpm)	Dissolution rate ($\text{mol m}^{-2} \text{s}^{-1}$)	Reference	(–) dr/dt ($\mu\text{m/min}^{-1}$)
Calcite	25	1	340	5.65E-03	1	12.52
	25	2	340	8.44E-04	1	1.87
	25	3	340	7.37E-05	1	0.16
	25	4	425	2.52E-05	2	0.06
	25	5	–	8.15E-06	3	0.02
	50	1	340	1.12E-02	1	24.82
	50	2	340	1.31E-03	1	2.90
	50	3	340	1.41E-04	1	0.31
	80	1	340	1.84E-02	1	40.66
	80	2	340	1.73E-03	1	3.82
	80	3	340	1.84E-04	1	0.41
	80	3	340	1.84E-04	1	0.41
Dolomite	25	1.1	500	2.28E-04	4	0.60
	25	2	500	4.37E-05	4	0.11
	25	3	500	9.62E-06	4	0.03
	25	4.1	500	2.40E-06	4	0.01
	25	5	–	7.94E-07	3	0.00
	50	1.1	500	8.53E-04	4	2.23
	50	2	500	1.46E-04	4	0.38
	50	3.05	500	2.84E-05	4	0.07
	50	4.1	500	3.94E-06*	4	0.01
	80	1.1	500	2.25E-03	4	5.87
	80	2.05	500	3.14E-04	4	0.82
	80	3.1	500	5.35E-05	4	0.14
	80	4.3	500	5.10E-06*	4	0.01
	80	4.3	500	5.10E-06*	4	0.01
Siderite	25	1	425	8.30E-06	5	0.02
	25	2	425	2.86E-06	5	0.01
	25	3	425	1.11E-06	5	0.00
	25	4	425	1.50E-07	5	0.00
	60	1.1	425	1.19E-04	5	0.21
	60	2.1	425	5.85E-05	5	0.10
	60	3.1	425	1.15E-05	5	0.02
	60	4.6	425	1.95E-07	5	0.00
	80	1.1	425	4.83E-04	5	0.85
	80	2.1	425	2.16E-04	5	0.38
	80	3.4	425	8.71E-06	5	0.02
	80	4.3	425	2.07E-06	5	0.00
	100	1.2	425	9.95E-04	5	1.75
	100	2.1	425	3.77E-04	5	0.66
	100	3.1	425	6.38E-05	5	0.11
	100	4.4	425	2.97E-06	5	0.01

The calculation of the critical radii as a function of pH and temperature is based on several assumptions: 1) particles are spherical, 2) conditions are far from equilibrium, implying that only forward rates of mineral dissolution as reported in literature are taken into consideration, and 3) constant change of the radius with time, which is a consequence of surface controlled dissolution of spherical particles.

The critical radii for the acid dissolution of the different carbonates was calculated for a defined time of 60 min. The investigated time period was a practical starting point for an extraction scheme that can be completed within 8 h. First, the temporal change of the radius with time (dr/dt) was calculated:

$$\frac{dr}{dt} = \frac{R^* M_w}{\rho} * 10^6 * 60 \quad (2)$$

where (dr/dt) is expressed in ($\mu\text{m}/\text{min}$), the dissolution rate (R) in $\text{mol m}^{-2} \text{s}^{-1}$, the mineral density (ρ) in g m^{-3} and the molar weight (M_w) in g mol^{-1} . The unit correction factors 10^6 and 60 correspond to the transformation of distance and time to μm and minutes, respectively.

The change in radius (Δr) in a defined time (1 h) is independent on the initial radius, and can be calculated based on the dissolution rate at given pH and temperature conditions by integrating the differential Eq. (2). The Δr is used to determine the critical radius of a particle by comparing the initial (r_i) and final (r_f) radius of a sphere.

$$r_i = \Delta r + r_f \quad (3)$$

The final radius related to 95% or 5% dissolution in a limited period of time is given by:

$$r_f = r_i * \sqrt[3]{Z} \quad (4)$$

where Z is the target percentage of mineral dissolution for defining the critical radius. Z is equal to 0.05 or 0.95 for 95% and 5% dissolution of the initial volume, respectively. Combining Eq. (3) and Eq. (4) yields the expression to calculate the critical radii corresponding to 95% and 5% dissolution of a spherical carbonate mineral.

$$r_i = \frac{\Delta r}{1 - \sqrt[3]{Z}} \quad (5)$$

The critical radii for the dissolution of calcite, dolomite and siderite as a function of pH and temperature are presented in Fig. 1. The acid dissolution of calcite is mainly dependent on pH with a negligible effect of temperature. The pH value is also the dominant factor controlling the acid dissolution of dolomite, but temperature is more important compared with calcite, especially with increasing pH. In contrast, the acid dissolution of siderite is highly dependent on both pH and temperature. Consequently, temperature is the key parameter for the separation of siderite from calcite and dolomite. Therefore, dissolution of calcite and dolomite can be best performed at low temperature (25 to 30 °C) in order to minimize the dissolution of siderite. In contrast, the dissolution of siderite has to be performed at elevated temperatures (>65 °C) in order to obtain quantitative dissolution within the envisioned time frame.

Carbonates such as calcite, dolomite and siderite are found predominantly in the silt fraction of sediments (Huisman, 1998; Boogs, 2009; Griffioen et al., 2016). The shaded area can be used to identify optimal conditions for separating the three carbonates within this grain size fraction. In Fig. 1A, the lower limit of the shaded area indicates that a pH of 2.75 is required to achieve $\geq 95\%$ dissolution of a calcite particle with a diameter of 63 μm at 30 °C within 1 h. Under such conditions, also dolomite and siderite spheres with diameters of below 8 and 0.7 μm , respectively, are expected to dissolve $>95\%$ (Fig. 1B and C). Only when dolomite and siderite particle have larger diameters than 270 μm and 20 μm respectively, they are expected to lose $<5\%$ of their mass under these conditions (Fig. 1b and c). Hence, according to the

model, separating dolomite from calcite in mixtures of silt size particles seems to be unfeasible within the practical constraints.

Furthermore, quantitatively separating calcite and dolomite from siderite requires other conditions. For dissolving dolomite particles of 63 μm , Fig. 1B indicates a minimum pH of 1.6 for dissolution of $\geq 95\%$ at 30 °C within 1 h. Under these conditions, siderite particles with a radius of 80 μm and larger are expected to lose $\geq 5\%$ of their mass. Based on these findings, selective dissolution of calcite or dolomite with minimum dissolution of siderite was tested at pH of 2.8 and 1.9, respectively, at 30 °C. Furthermore, after dissolving calcite and dolomite, quantitative dissolution of siderite should be achieved within 3 h at pH 0 and 80 °C.

3. Materials and methods

3.1. Standards and samples

Natural samples of calcite, dolomite and siderite were obtained from the sample collection used for the development of the Atlas of Electron Microscopy of Clay Minerals and Their Admixtures (Beutelspacher and Van der Marel, 1968) and the Atlas of Infrared Spectroscopy of Clay Minerals and Their Admixtures (Van der Marel & Beutelspacher, 1976), other mineral samples were purchased from WARDS Natural Scientific (Table 2). The correctness of the description of the reference materials was verified by XRD using a Bruker D2 instrument equipped with a Co tube. Some of the reference materials contained minor amounts of quartz (Table 2). Besides quartz, no other crystalline materials than the indicated carbonates were identified in the diffractograms. Elemental composition of the carbonate samples was determined after 7 days digestion in 1 M HCl followed by ICP OES analysis of the solution using a SPECTRO ARCOS instrument (Analytical Instrument GmbH). Metals, which were present in concentrations above 0.10% dwt were included in the stoichiometry of the carbonate in Table 2. In calcite samples 2 and 3, Mg concentrations were about 0.06 and 0.08% dwt, respectively. Strontium concentrations varied between 0.01 and 0.04% dwt. The concentrations of all other analysed trace elements (such as Fe, Mn and Ba) were below the detection limit of the instrument corresponding to elemental contents of about 0.001 to 0.007% dwt in the solids. The uncertainty of elemental concentration based on repeated measurements of reference materials is about 2%.

All carbonate samples were acid washed with 1 M HCl for 2 to 5 h to remove all impurities from the mineral surfaces and later rinsed with UHQ purged with Ar gas for 3 h prior to use. This was done to remove dissolved oxygen in order to prevent oxidation of siderite. The washing of siderite was performed in a glove box under N_2/H_2 95%/5% atmosphere. To represent the typical size fraction of carbonates in nature, all mineral standards were grinded in an agate mortar and sieved to $<63 \mu\text{m}$. Clay-size particles were removed by centrifugation according to the method of Soukup et al. (2008). Afterwards, the samples were freeze dried and sieved again.

The optimized sequential extraction for carbonates established in this study was tested on sediment samples and rocks from a diverse array of environments and ages (Table 3). The sediment samples were freeze dried and stored under Ar atmosphere at 4 °C. The siderite concretion was cut in half and a subsample was taken from the cut phase by drilling. The collected siderite material was stored under Ar atmosphere at 4 °C until extraction. The core from the banded iron formation (BIF) was collected during the 1990's; it was subsampled in 2014 and stored under atmospheric conditions until analysis.

3.2. Reagents

All solutions were prepared using boiled and degassed UHQ water and all reagents were analytical grade. The UHQ was heated at 200–250 °C and boiled for 3 h. Later the warm water was exposed to partial vacuum until degassed. The solutions were prepared in a glovebox under CO_2 free N_2/H_2 95%/5% atmosphere and placed in syringes closed

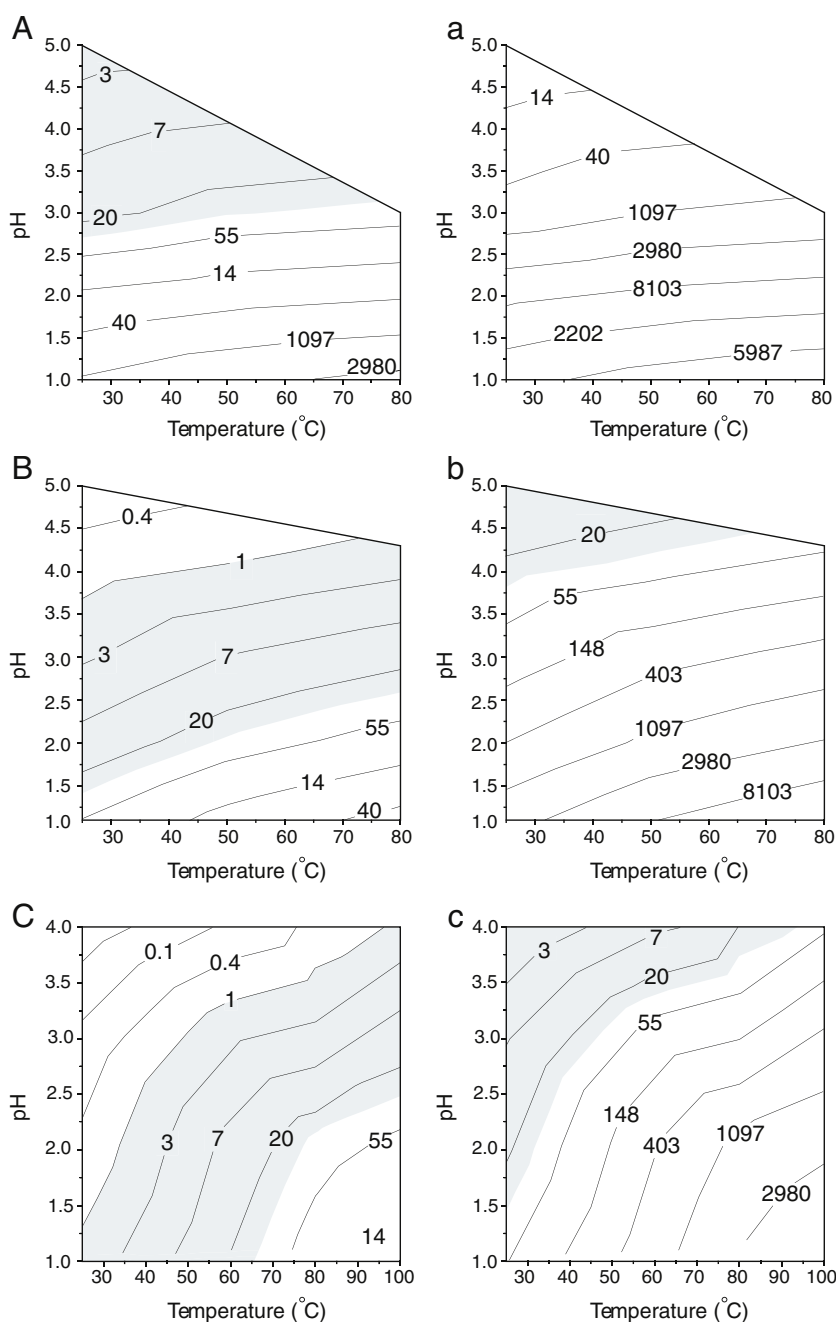


Fig. 1. Results from the theoretical survey of extraction conditions. Effect of pH and temperature on the critical particle radius related to 95% (A, B, C) and 5% (a, b, c) dissolution in 60 min for calcite (A, a), dolomite (B, b) and siderite (C, c). The particle size is represented as the particle radius (μm). The shaded area corresponds to the silt fraction.

with a Luer lock closure cap, prior to use to prevent any CO_2 contamination.

All glassware was washed and then treated with 2% HNO_3 for 24 h and subsequently rinsed at least 3 times with UHQ water. The following

solutions were used: 0.40 M sodium chloroacetate/0.16 M HCl adjusted to pH 2.8 with HCl for calcite dissolution and 0.30 M maleic acid/0.15 M NaCl adjusted to pH 1.9 with CO_2 -free 10 M NaOH for dolomite digestion. Siderite digestion was carried out by adding 32% HCl to the

Table 2

Reference materials used for testing the extraction method.

Sample	Elemental composition	Location	Description
Cal. 1	$\text{Ca}_{0.99}\text{Mg}_{0.01}\text{CO}_3$	Portland, Dorset, England	Calcite oolite with $\leq 4\%$ quartz
Cal. 2	CaCO_3	Arizona, USA	Calcite with traces of quartz
Cal. 3	CaCO_3	Chihuahua, México	Ward's specimen, Icelandic spar.
Dol. 1	$\text{Ca}_{0.49}\text{Mg}_{0.49}\text{Fe}_{0.01}(\text{CO}_3)_2$	Florence, Vermont, USA	Dolomite with $\leq 5\%$ quartz
Dol. 2	$\text{Ca}_{0.50}\text{Mg}_{0.47}\text{Fe}_{0.03}(\text{CO}_3)_2$	Ontario, Canada	Dolomite with traces of quartz
Sid. 1	$\text{Fe}_{0.84}\text{Mg}_{0.09}\text{Mn}_{0.05}\text{Ca}_{0.02}\text{CO}_3$	Steiermark, Austria	Siderite with traces of quartz
Sid. 2	$\text{Fe}_{0.75}\text{Mg}_{0.07}\text{Mn}_{0.16}\text{Ca}_{0.02}\text{CO}_3$	Queensdown, Quebec, Canada	Ward's specimen, research grade siderite

Table 3

Natural sediment and rock samples used for the testing of the extraction procedure described in this study.

Sample	Location	Environment
Fluv-clay	Waalre Formation, Limburg, The Netherlands	Fluvial clay-rich sediment
Concretion	Waalre Formation, Limburg, The Netherlands	Siderite-rich concretion
Mar-clay	Rupel Clay, Limburg, The Netherlands	Marine clay-rich sediment
Mar-sand	Coastal nourishment project Sand motor, South Holland, The Netherlands	Marine sand-rich sediment
Mar-mud	Black Sea	Marine mud-rich sediment
Brack-clay	Bothnian Sea	Brackish clay-rich sediment
BIF-rock	Iron banded formation, South Africa	Metamorphic rock

chloroacetate and maleate buffers. The trapping solutions were 0.10 M AgNO_3 /0.15 HNO_3 for trapping H_2S and 0.10 M NaOH prepared from Titrisol® solutions for trapping CO_2 . For carbon isotope analysis the CO_2 -was precipitated in a 1.7 M BaCl_2 solution.

3.3. Apparatus

The experimental setup consists of two parts: the reaction and the trapping sections (Fig. 2). The reactor is a 250 ml 3-neck glass flask with a flat bottom. The central neck (ST/NS 12/21) was connected to a 10 cm long condenser while one of the side necks (ST/NS 14/23) served as an injection and sampling port. The injection and sampling port consisted of a glass arm (ST/NS 14/23) closed with a lid containing a hole (GL 12) and a silicon ring, in order to adapt and seal a plastic tube and the connector coupled to a three-way valve. The third neck (ST/NS 14/23) was used as a connection to an Ar gas reservoir made of airtight PETP/Al/PE three-layer foil bag, which was used to purge the reactor. A reservoir was used in order to minimize pressure differences between the inside of the reactor and the outside, which could induce a loss or the contamination of the gas flowing through the reactor. The reactor was placed in a temperature controlled oil bath, which was installed on a stirring hot plate (Ika RCT). Temperature in the oil bath was measured and maintained constant using an electronic contact thermometer (Ika ETS D5). Stirring of the suspension in the reactor was performed by a magnetic stir bar. Stirring was necessary to generate a well-mixed sediment suspension and to minimize the transport limitation.

The gas flow through the reactor was controlled at the connection between the reactor and the trapping tubes by a Masterflex L/S Cartridge pump set at 27 ml/min using Masterflex L/S 14 C-flex tubing.

Tygon R3603 (ID 1.6 mm, OD 4.8 mm, WT 1.6 mm) tubing was used for all other connections (Fig. 2). The pump ensures a regular and constant flow of gas from the reactor towards the trapping solutions. The first trap contained 40 ml of the AgNO_3 solution. This trap was followed by two traps filled with 40 ml of the NaOH trapping solution, followed by an empty tube and a water lock. The empty tube was added to prevent mixing of water and trapping solution in the case of generating backpressure when sampling the trapping solutions. The trapping tubes were fabricated of glass and closed with Pyrex® 22 screw-caps with a hole and closed with 2 silicone stoppers. These stoppers were perforated to tightly fit PA tubing (ID 4 mm and OD 6 mm) and the respective connections and sampling port.

3.4. Procedure for the optimized sequential extraction

The procedure for separation, quantification and characterization of siderite described here comprises the sequential digestion of calcite/siderite and dolomite/siderite mixtures through acid dissolution, and subsequent retrieval of the evolved CO_2 and finally precipitation of BaCO_3 for the carbon isotope analysis. The conditions of time and temperature set in the following scheme were pre-tested with pure and mixtures of calcite, dolomite and siderite (Table 2). The following protocol was used for the recovery of the CO_2 and sampling of the concomitant solution (Fig. 3):

- Weigh the dried sample based on total inorganic carbon content. The recommended minimum inorganic carbon content in the reactor is 1.4 mg C or 10 mg of carbonates. Roll a pergamyn paper (100 × 100 mm), insert it as a funnel in one of the necks of the reactor and add the sample. Add the stirring bar and lubricate the joints of the reactor with silicone grease, proceed to place the reactor into the oil bath. Connect the reaction vessel to the condenser, the Ar reservoir and the injection/sampling port.
- Set the thermometer at 30 °C and the pump at 27 ml/min.
- Add the AgNO_3 solution to the first trapping tube and make sure that all the connections are air tight by using a leak detector spray.
- Generate a partial vacuum in the reaction flask by pumping gas out of the flask for 15 min with the main Ar gas inlet closed, in order to remove a considerable portion of air from the reaction flask and avoid siderite oxidation.
- Open the Ar gas inlet and flush the reaction vessel for 1 h with Ar gas by continuously pumping the gas from the reaction flask.
- Turn off the pump and flush the trapping tubes with Ar gas from the secondary Ar inlet for 10 min at high gas flow

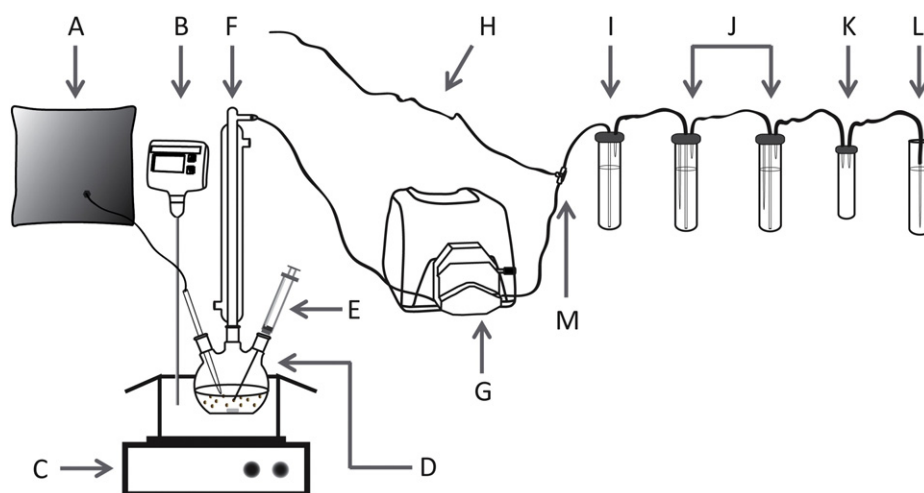


Fig. 2. The experimental setup used for the sequential extraction for carbonates: (A) Ar gas reservoir (main Ar gas inlet), (B) thermometer, (C) hot plate, (D) reaction flask, (E) injection and sampling port, (F) condenser, (G) peristaltic pump, (H) secondary Ar inlet, (I) AgNO_3 trap, (J) NaOH trap, (K) empty tube, (L) water lock and (M) three-way valve.

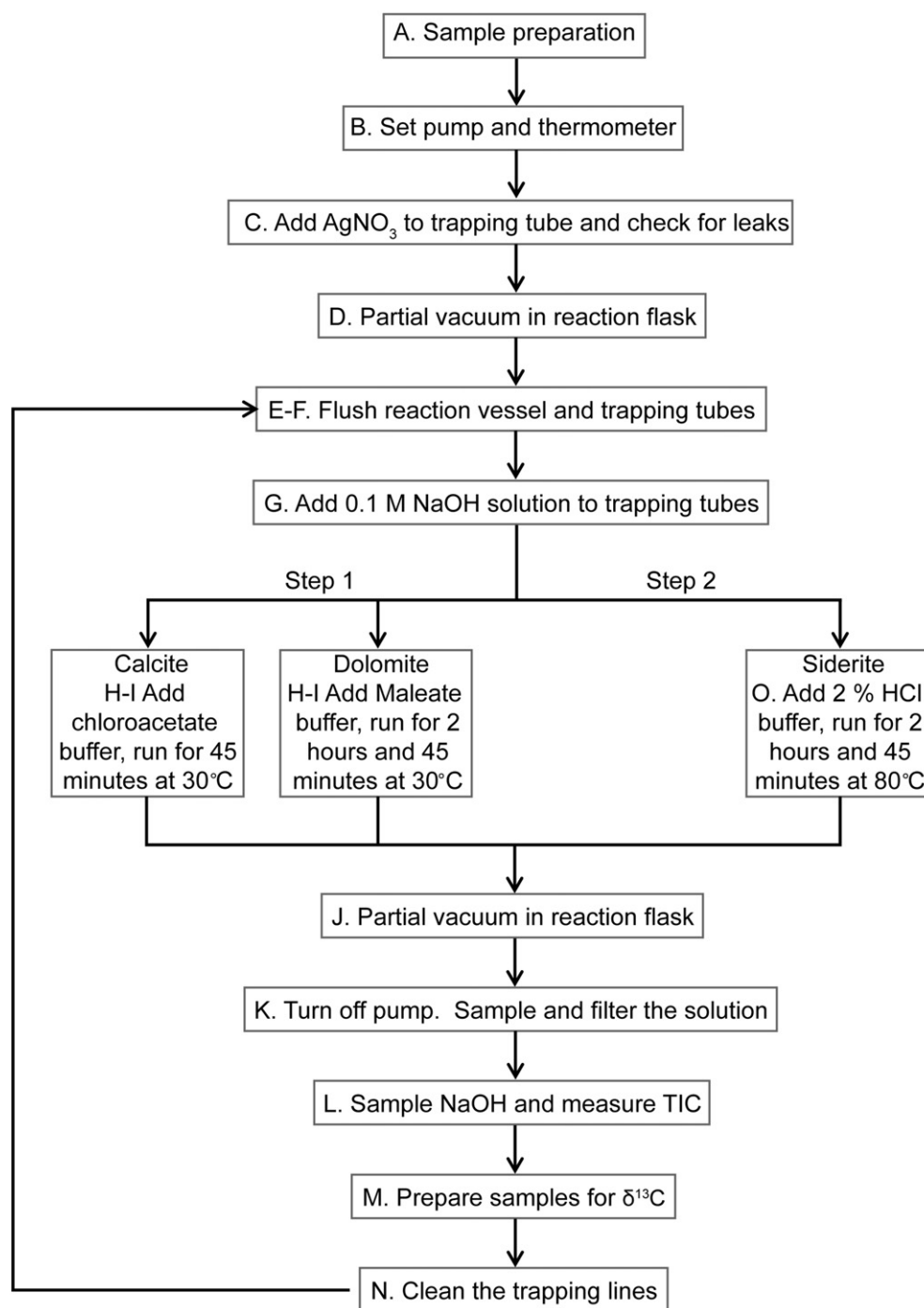


Fig. 3. Scheme of optimized sequential extraction for carbonates.

(~40 ml/min) to remove all remaining air from the empty trapping tubes.

- G. Flush the opening of the three-way valve coupled to the sampling port of the CO₂ trapping tubes with Ar gas, quickly place the syringes filled with 40 ml of 0.1 M NaOH and fill the solutions into the trapping tubes while purging the tubes with Ar gas.
- H. Close the secondary Ar inlet and start pumping the reactor with the main Ag gas inlet open. Proceed to inject 50 ml of the buffer (chloroacetate buffer for samples only containing calcite or maleate buffer for dolomite containing samples) to the reactor via the injection and sampling port. Start stirring at 900 rpm.
- I. Purge the reactor with inert gas by pumping the gas phase with a rate of 27 ml/min and channelling the gas through the traps for

the desired time (calcite: 45 min and combined calcite/dolomite: 2 h and 45 min).

- J. Create a partial vacuum in the reaction flask by pumping the gas phase towards the traps for 15 min with the main Ar gas inlet closed, to ensure a ≥ 95% recovery of the released CO₂.
- K. Stop the pump and the stirring, sample the reactor solution through the port, and filter it immediately.
- L. Flush the trapping tubes by opening the secondary Ar gas inlet to sample the trapping solutions. Place 5 ml syringes in the sampling ports of the trapping tubes and sample 4 ml for total inorganic carbon (TIC) measurement. Purge the TIC sampling tubes with inert gas to flush the air present in the tubes to avoid CO₂ contamination. Immediately add 4 ml of the NaOH solution

into the tubes and close them tightly. The NaOH solution must be quickly measured to avoid any CO₂ contamination from air.

- M. Add 3 ml of 1.7 M BaCl₂ to each NaOH trap to prepare the isotope samples. Let the BaCO₃ precipitate in the tube. This suspension must be filtered under Ar gas atmosphere with a 47 mm Ø glass microfiber filter. Dry the filter at 60 °C for at least 12 h.
- N. Remove and clean all trapping tubes and connections. Continue by placing new trapping tubes and ensure that all parts are leak-free. Repeat steps F and G.
- O. Restart the experiment by turning on the pump in order to dissolve the siderite present in the sediment sample. Add 10 ml of 32% HCl to the reaction vessel, start stirring at 900 rpm and pump the gas phase towards the trapping solutions for 3 h.
- P. Repeat the steps J until M to complete the extraction procedure.

3.5. Extent of mineral dissolution and gas phase recovery

The extent of mineral dissolution during the digestion of the different reference carbonates was assessed based on solution composition. The total amounts of added carbonates were calculated based on their stoichiometry (Table 2) using the cation concentrations in solution after complete digestion of the added minerals. The concentrations of cations were measured by ICP OES (SPECTRO ARCOS, Analytical instrument GmbH). The CO₂ recoveries were calculated based on the TIC content of the traps, measured with a Shimadzu TOC-5050A analyser. The standard deviation of triplicate TIC measurements was below 2%.

The Fe(II) extracted from both extraction steps was corrected for Fe coming from Fe-bearing Al silicates. When natural sediments are exposed to acidic conditions, Fe(II) might become released from silicate phases, in particular from clay minerals. Hence, the measured Fe(II) concentration was corrected based on the dissolved Al concentration in the solution. For this the Fe:Al ratio of the upper continental crust of 0.23 (Rudnick & Gao, 2003) was used. This ratio is close to the Fe:Al ratio (~0.25) of common clays such as illite and some 2:1 clay minerals.

3.6. Isotope analysis

The $\delta^{13}\text{C}$ composition of the reference materials were determined using a vacuum line (McCrea, 1950). The carbonates samples and H₃PO₄ (102%) were placed in two-legged vessels. These vessels were later sealed, evacuated and allowed to dry overnight. Later, the vessels were disconnected from the vacuum line and the acid was combined with the carbonates for the acid digestion to take place. The vessels were placed in a water bath for the time and temperature recommended by McCrea (1950) and Rosenbaum & Sheppard (1986) for the corresponding carbonates. Once the reaction was completed, the vessels were again connected to the vacuum line. Two cold traps were used, a cooled acetone trap (−80 °C) collected the water formed during the reaction and a second trap with liquid nitrogen was used to collect the released CO₂. The CO₂-containing vessels were connected to a VG SIRA-24 EM isotope ratio mass spectrometer for $\delta^{13}\text{C}$ analyses. The $\delta^{13}\text{C}$ obtained from BaCO₃, which was obtained from the CO₂ traps of the extraction line, was analysed with a Gas Bench-II (Thermo Fisher Scientific) following the method described by Spötl & Vennemann (2003): 102% H₃PO₄ was injected into an individual sample vial containing the sample and filled with helium and was allowed to react for 90 min at 70 °C. The formed CO₂ was sampled from the headspace as a continuous flow into a Delta-V IRMS (Thermo Fisher Scientific). In both methods the same standards were used. The internal standard NAXOS was used, which is a grinded marble material, calibrated versus NBS-19 and NBS-18. Also a BaCO₃ standard was used. The vacuum line was only used when a small number of samples had to be analysed and the Gas Bench was oversubscribed. Using the vacuum line is more time consuming than using the Gas Bench.

4. Results and discussion

4.1. Recovery of carbonate standards in the various extraction steps

The suitability of the reaction conditions as established from the theoretical considerations for the separation of the three carbonates, was evaluated by investigating the dissolution kinetics of individual carbonate minerals at these conditions. This was done by monitoring the Fe, Ca and Mg concentrations in solution (Fig. 4).

Potential release of CO₂ from the organic acids was tested by reacting the buffer solutions (chloroacetate and maleate) and 1 M HCl for 3 h at 80 °C without solid sample. The TIC concentrations in the NaOH trapping solutions of the blank extractions with 1 M HCl, chloroacetate and maleate solutions with a pH ~ 0 were 0.61 ± 0.24 , 0.73 ± 0.32 and 0.84 ± 0.25 mg C/L, respectively. This indicates that the release of inorganic carbon of the blank extractions is negligible.

Calcite standards were completely dissolved within ~20 min with the chloroacetate buffer at pH 2.8 and 30 °C. More than 95% of the dolomite was dissolved after reacting 150 min with the maleate solution at pH 1.9 and 30 °C. For dolomite, the standard deviation in the initial state of the reaction was larger compared to the other carbonates. We ascribe these variations to differences in particle size distribution of the dolomite aliquots which were added in the various experiments.

Most important for the extraction method, practically complete dolomite dissolution was achieved after 150 min reaction time in all experiments irrespective of the reaction progress in the initial state. At 30 °C, <5% and 11% of siderite were dissolved in solutions of chloroacetate at pH 2.8 after 1 h and, in maleate solutions at pH 1.9 after 3 h, respectively (Fig. 4 and Table 4). Siderite dissolved completely within 150 min during reaction at 80 °C and pH ~ 0 with both organic solutions. These results confirm that the preselected conditions based on the theoretical considerations are principally suitable for separating siderite from other carbonates. Nevertheless, the time required for the quantitative dissolution of the different carbonates deviated somewhat from the model predictions. When compared to the theoretical model, calcite standards dissolved faster under the presented conditions. In contrast, the required time for complete dissolution of dolomite and siderite exceeded the time predicted by the model. These time deviations can be attributed to the assumptions of the idealized model, in particular assuming spherical particle shape.

When including CO₂ trapping, the extraction had to be proceeded after complete dissolution of the minerals, due to the time required for transferring the released CO₂ from the reactor into the gas traps. More than 95% of the CO₂ was recovered from calcite dissolution with a 0.4 M chloroacetate buffer at pH 2.8 and 30 °C after 60 min (Table 4). For dolomite, extraction with 0.3 M maleate buffer at pH 1.9 at 30 °C for 3 h was sufficient to reach a recovery of ≥95%. The separation

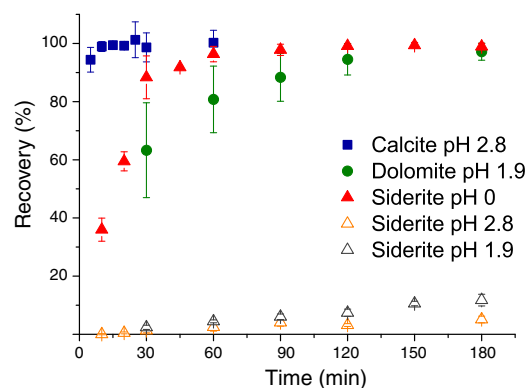


Fig. 4. Progression of the acid dissolution of calcite with a chloroacetate buffer, dolomite with a maleate buffer and siderite with both buffers and at pH ~ 0 after adding 32% HCl. The bars represent the standard deviation of the recovery of triplicate extraction experiments.

Table 4

Recovery of calcite, dolomite and siderite for the optimal extracting conditions. The average recoveries and the corresponding standard deviation are calculated from triplicate extractions.

Mineral	Temperature (°C)	pH	Time (min)	Mass added (mg)	Recovery (wt%)
Cal. 1	30	2.8	60	15.8–18.1	99 ± 4
Cal. 2	30	2.8	60	16.2–20.5	97 ± 3
Cal. 3	30	2.8	60	11.0–11.9	102 ± 5
Dol. 1	30	1.9	180	11.8–14.1	100 ± 1
Dol. 2	30	1.9	180	10.8–29.0	95 ± 1
Sid. 1	30	2.8	60	20.7–39.3	4 ± 1
Sid. 2	30	2.8	60	13.8–30.2	5 ± 1
Sid. 1	30	1.9	180	28.0–42.5	11 ± 1
Sid. 2	30	1.9	180	19.4–20.1	9 ± 1
Sid. 1	80	0	180	14.4–20.4	97 ± 1
Sid. 2	80	0	180	19.0–37.9	97 ± 2

of calcite and dolomite was attempted. However, as concluded theoretically, the variability of grain sizes of the carbonates makes it impossible to quantitatively digest calcite without dissolving a considerable fraction of dolomite. Based on CO₂ recovery, ~5% to ~11% of the carbonate bound to siderite was extracted under the conditions for calcite and dolomite digestion, respectively. These fractions are in agreement with the expectations based on the model calculations. When reacting siderite at pH ~0 and 80 °C for 3 h, ≥97% of the CO₂ was recovered in the gas traps.

4.2. Isotope calibration

The measured $\delta^{13}\text{C}$ of the BaCO₃ collected after the extraction steps ($\delta^{13}\text{C}_E$) deviated from the value obtained by $\delta^{13}\text{C}$ analysis of the pure reference materials (Table 5). These differences can be explained by a mass bias of the procedure. However, the shift in isotopic signature is linear and therefore a calibration line was built based on the relationship between the actual $\delta^{13}\text{C}$ of the carbonate standards analysed directly without using the set-up for sequential extraction and $\delta^{13}\text{C}_E$ after digestion with the optimized extraction solutions. The linear regression equation obtained from the entire data in Table 5 resulted in the following empirical relationship (with r^2 equal to 0.993).

$$\delta^{13}\text{C} = \delta^{13}\text{C}_E * 1.15 + 3.69 \quad (6)$$

The influence of the material with extremely light $\delta^{13}\text{C}$ value (−43.2‰) on the regression equation was evaluated by comparing empirical regression lines with and without this extreme value. The maximum difference between calculated $\delta^{13}\text{C}$ values in the analysed range with both regression lines was 0.5‰. All reported $\delta^{13}\text{C}$ values have been calculated from the $\delta^{13}\text{C}_E$ values using Eq. (6).

4.3. Recovery of CO₂ and $\delta^{13}\text{C}$ values obtained from mixtures of carbonate standards

The capability of the method to separately dissolve the different carbonates and to determine their individual $\delta^{13}\text{C}$ signatures was tested

Table 5

Results from measuring $\delta^{13}\text{C}$ values of reference materials. Corrected $\delta^{13}\text{C}$ values were calculated using Eq. (6). Averaged $\delta^{13}\text{C}$ values and standard deviations are presented from triplicate extractions.

Sample	$\delta^{13}\text{C}\text{‰ PDB}$	$\delta^{13}\text{C}\text{‰ PDB}$ measured	$\delta^{13}\text{C}\text{‰ PDB}$ corrected
Naxos standard	2.10 ± 0.12	−0.65 ± 0.60	2.95 ± 0.68
Gas Bench standard	−43.20 ± 0.04	−39.84 ± 2.01	−42.08 ± 2.18
Cal. 2	−5.21 ± 0.40	−8.56 ± 0.36	−6.14 ± 0.42
Cal. 3	2.86 ± 0.05	−0.86 ± 0.05	2.71 ± 0.05
Dol. 1	−0.27 ± 0.04	−3.27 ± 0.10	−0.06 ± 0.12
Dol. 2	−8.29 ± 0.41	−10.07 ± 0.13	−7.88 ± 0.15
Sid. 1	−12.15 ± 0.18	−14.22 ± 0.20	−12.64 ± 0.23
Sid. 2	−5.63 ± 0.03	−7.74 ± 0.61	−5.20 ± 0.70

with several mixtures of calcite/siderite and dolomite/siderite under the conditions described in the section above (Table 6). The calcite/siderite mixtures showed recoveries ≥95% in both fractions, implying that quantitative separation was achieved. The extent of siderite dissolution in the calcite step was smaller in the presence of calcite than when reacting under the same conditions without calcite. This suggests that siderite dissolution may be retarded by the presence of Ca²⁺ ions released from the dissolution of calcite. As expected, the amount of carbonate released from dolomite in the dolomite/siderite mixtures was overestimated by ~13%, while the corresponding siderite content was underestimated by ~14%. That is because a part of the siderite-bound carbonate contributed to the CO₂ recovered in the dolomite extraction step. The measured $\delta^{13}\text{C}$ value of calcite was not significantly different from that obtained for the isolated material (Table 6). For siderite, a $\delta^{13}\text{C}$ difference of 1.4‰ was found. The $\delta^{13}\text{C}$ measured for dolomite showed a difference of 1.1‰ with respect to the value obtained from the pure material as a consequence of the overestimation of siderite in the first extraction step; while a negligible difference of 0.03‰ was determined for the $\delta^{13}\text{C}$ of siderite. In order to rectify for this deviation in $\delta^{13}\text{C}$, a straightforward correction can be done using the measured $\delta^{13}\text{C}$ signatures and the cation concentrations present in the solution during the first extraction step.

$$\delta^{13}\text{C}_{\text{Carb1}} = \frac{\text{TIC}_{\text{Mix1}} * \delta^{13}\text{C}_{\text{Mix1}} - \text{TIC}_{\text{Sid}} * \delta^{13}\text{C}_{\text{Sid}}}{\text{TIC}_{\text{Carb1}}} \quad (7)$$

where $\delta^{13}\text{C}_{\text{Carb1}}$ denotes the $\delta^{13}\text{C}$ signature of calcite or dolomite extracted in the first step, $\delta^{13}\text{C}_{\text{Mix1}}$ is the $\delta^{13}\text{C}$ signature obtained in first extraction step, the $\delta^{13}\text{C}_{\text{Sid}}$ corresponds to the $\delta^{13}\text{C}$ signature of siderite obtained from the last extraction step. TIC_{Mix1}, TIC_{Sid} and TIC_{Carb1} in mmol/g are the total TIC, TIC from siderite and TIC content of calcite or dolomite in the first extraction step, respectively. TIC_{Sid} and TIC_{Carb1} are calculated based on the concentrations of Fe(II), Ca and Mg in the reactor solution.

For calcite, the difference in $\delta^{13}\text{C}$ between the pure calcite and the $\delta^{13}\text{C}$ value obtained from the extraction increased upon correction using Eq. (7) (Table 6). This increase could be attributed to fractionation during extraction. Walters et al. (1972) reported that first-reacting calcite during acid solution was about 3‰ lighter than the bulk phase. This trend, however, cannot explain why the $\delta^{13}\text{C}$ value of calcite in the mixture is higher than expected because co-dissolution of siderite should lead to lower $\delta^{13}\text{C}$ values, in this case. Hence, the larger difference in the $\delta^{13}\text{C}$ values of calcite between measured and expected values after correction by Eq. (7) remains enigmatic. Nevertheless, the deviation, with and without correction, remained at a level below 1‰. The relative amount of siderite dissolving during the calcite extraction step, when using the chloroacetate buffer, is very low and correcting of the small contribution of siderite-derived CO₂ in the calcite extraction step is unnecessary. Correcting $\delta^{13}\text{C}$ values of carbonates, which are extracted in the first step, becomes relevant when the contribution of siderite-derived CO₂ is larger. This is the case when using the maleate buffer for

Table 6

Recovery and $\delta^{13}\text{C}$ measurements obtained from mixture of reference materials after calculation with Eq. (6). The step 1 (S₁) corrected $\delta^{13}\text{C}$ values were calculated with Eq. (7). The $\delta^{13}\text{C}$ difference is the deviation between S₁ corrected (*) and measured $\delta^{13}\text{C}$ value with respect to the $\delta^{13}\text{C}$ value obtained from analysing the pure reference carbonates.

Mineral mixture	Mass added (mg)	Recovery (%)	Measured $\delta^{13}\text{C}$ (‰ PDB)	S ₁ corrected $\delta^{13}\text{C}$ (‰ PDB)	$\delta^{13}\text{C}$ difference (‰ PDB)
Calcite/siderite					
Cal. 3	11.9–15.0	97 ± 2	2.98 ± 0.20	3.50 ± 0.20	0.11 (*0.64)
Sid. 2	11.0–13.9	99 ± 2	−4.18 ± 0.26		1.45
Dolomite/siderite					
Dol. 2	12.6–18.1	113 ± 1	−7.17 ± 0.96	−7.81 ± 0.98	1.12 (*0.41)
Sid. 2	16.5–19.5	86 ± 2	−5.59 ± 0.35		0.03

dolomite extraction. In this case, the difference between $\delta^{13}\text{C}$ values of dolomite in the mixture and the value obtained from isolated extraction improved from 1.12‰ to 0.41‰. Considering the typically large difference of $\delta^{13}\text{C}$ signatures of diverse sources for carbonates, in the order of tens of per mill, the $\delta^{13}\text{C}$ offsets between the pure minerals and the results obtained with the optimized sequential extraction in the mixtures are acceptable in many applications. The advantage of the method is that it permits to quantify the different carbonate phases using both the solution composition and the released gases. This, in turn, opens the possibility to correct the $\delta^{13}\text{C}$ values regarding the simultaneous dissolution of different phases during digestion.

4.4. Application to sediment samples

The extraction was tested on a diverse group of sediment and rock samples (Table 7). For some sediment samples, the siderite content calculated based on dissolved Fe(II) concentration had the tendency to be higher than the value calculated from the recovered CO_2 . It is very likely that this overestimation originates from stoichiometric variations in the siderite and by partial dissolution of Fe-bearing Al-silicates present in the samples such as biotite and chlorite. These minerals have a higher Fe/Al ratio than the ratio used in the correction. Calcite and dolomite mixtures can be identified by Ca and Mg concentrations in the extraction solution of the dolomite step of the fluvial-clay, the marine-sand and the marine-mud samples. Also, the extraction solution for the fluvial-clay and the BIF rock samples indicate partial dissolution of ankerite. This was corroborated by XRD data of these samples. The $\delta^{13}\text{C}$ values obtained from the BIF sample ($\sim -10\text{‰}$) are in good agreement with the reported $\delta^{13}\text{C}$ in literature (-9 to -12‰) (Becker and Clayton, 1972; Craddock and Dauphas, 2011).

In sediment samples with very high Fe carbonate and low calcite or dolomite content, such as fluvial-clay and the BIF rock, dissolution of a small fraction of the siderite during the calcite or dolomite extraction steps can lead to a considerable overestimation of the calcite and dolomite content based on the amount of released CO_2 .

Samples from the Bothnian Sea and the Black Sea show high discrepancies in the siderite content when calculated from the recovered CO_2 and from the released Fe(II): presence of siderite is indicated based on the release of Al-corrected Fe(II) in the solution but practically no CO_2 was recovered. This emphasizes the importance of simultaneously determining the solution composition and the CO_2 release to avoid misinterpretation when only one of the components is detected. The Bothnian Sea sample showed precipitation of AgS in the AgNO_3 trap

when performing the extraction. This indicates that dissolution of Fe sulphides had contributed to the Fe (II) release into solution. This is in agreement with the conclusions by Egger et al. (2015) based on sequential extractions of these sediments. They used the extraction scheme from Poulton & Canfield (2005) and detected about 3 wt% Fe-carbonates, but they concluded that the detection of Fe-carbonates was an artefact due to the high AVS content in these sediments. This observation shows that positive identification of minerals phases using two lines of evidence should be preferred over a single line of evidence for extraction procedures.

5. Conclusions

An optimized method is established that allows the quantification and characterization of different carbonates in both recent and ancient materials. Results from testing the method confirm the theoretical considerations, which indicate that the variability of grain size poses a challenge to separating different carbonate minerals despite intrinsic different reactivity. Separation of dolomite and calcite is not possible with acceptable uncertainty in the investigated range of pH and temperature conditions. Suitable conditions were identified for optimum separation of siderite and Ca/Mg carbonates.

Our results demonstrate the importance of measuring dissolved and volatile components when performing sequential extractions targeting carbonates or sulphides. Quantification of the dissolved ions is necessary for evaluating the specificity of the method, to ensure quantitative recovery of the released CO_2 (or H_2S) and can be used to correct measure isotopic signatures.

Acknowledgements

The research described is part of a research project on reactive Fe minerals in Dutch fluvial and marine sediments and financially supported by TNO Geological Survey of the Netherlands. The authors acknowledge D. van de Meent, H. de Waard, T. Zalm and A. van Dijk for their technical and analytical support. We thank the editor for his careful review of the paper and support, and the three anonymous reviewers for their insightful comments.

References

- Al-Aasam, I.S., Taylor, B.E., South, B., 1990. Stable isotope analysis of multiple carbonate samples using selective acid extraction. *Chem. Geol.* 80 (2), 119–125 (Isotope Geoscience section).

Table 7

Content of various carbonates in natural sediments and rocks expressed in terms of carbon content obtained from the extraction procedure. In the first extraction step either the procedure for dolomite or calcite extraction was used. The released CO_2 in the extraction step was used to calculate the corresponding carbonate content and $\delta^{13}\text{C}$ values after correction with Eq. (7). Additionally, the content of the various carbonates was estimated based on the release of ions into solution. Values below detection limit (total amount of added C < 1.4 mg) are indicated by <DT. All extraction analyses were performed in duplicates and the errors reflect the observed data range.

Sample	Step	Gas phase		Solution			
		Carbon (wt%)	$\delta^{13}\text{C}$ (‰)	Calcite (C wt%)	Dolomite (C wt%)	Siderite (C wt%)	Ankerite (C wt%)
Fluvial-clay	Dolomite	2.80 ± 0.06	1.56 ± 0.25	1.60 ± 0.03	1.08 ± 0.02	0.55 ± 0.02	0.20 ± 0.01
	Siderite	0.44 ± 0.01	−9.53 ± 0.27				
Concretion	Calcite	0.93 ± 0.02	−12.16 ± 0.63	0.19 ± 0.04		6.24 ± 0.16	0.89 ± 0.07
	Siderite	6.57 ± 0.13	−11.80 ± 0.73				
Marine-clay	Calcite	0.99 ± 0.02	−3.40 ± 0.72	0.92 ± 0.04		0.15 ± 0.02	
	Siderite	0.11 ± 0.01	−12.71 ± 0.15				
Marine-sand	Dolomite	1.46 ± 0.03	−0.19 ± 0.24	1.47 ± 0.03	0.31 ± 0.00	0.02 ± 0.00	
	Siderite	<DT					
Marine-mud	Dolomite	0.89 ± 0.02	1.61 ± 0.16	0.85 ± 0.01	0.29 ± 0.00	0.36 ± 0.02	
	Siderite	<DT					
Brackish-clay	Calcite	<DT		0.05 ± 0.00		0.20 ± 0.08	
	Siderite	<DT					
BIF-rock	Calcite	1.18 ± 0.02	−9.37 ± 0.34	0.37 ± 0.00		6.21 ± 0.05	0.43 ± 0.02
	Siderite	5.70 ± 0.11	−10.51 ± 0.18				

- Albani, A.E., Vachard, D., Kunt, W., Thurow, J., 2001. The role of diagenetic carbonate concretions in the preservation of the original sedimentary record. *Sedimentology* 48 (4), 875–886.
- Alkattan, M., Oelkers, E.H., Dandurand, J.-L., Schott, J., 1998. An experimental study of calcite and limestone dissolution rates as a function of pH from -1 to 3 and temperature from 25 to 80 °C. *Chem. Geol.* 151 (1–4), 199–214.
- Alkattan, M., Oelkers, E.H., Dandurand, J.-L., Schott, J., 2002. An experimental study of calcite dissolution rates at acidic conditions and 25 °C in the presence of NaPO_3 and MgCl_2 . *Chem. Geol.* 190 (1–4), 291–302.
- Amirbahman, A., Schöenberg, R., Johnson, C.A., Sigg, L., 1998. Aqueous- and solid-phase biogeochemistry of a calcareous aquifer system downgradient from a municipal solid waste landfill (Winterthur, Switzerland). *Environ. Sci. Technol.* 32 (13), 1933–1940.
- Antoniou, E.A., van Breukelen, B.M., Putters, B., Stuyfzand, P.J., 2012. Hydrogeochemical patterns, processes and mass transfers during aquifer storage and recovery (ASR) in an anoxic sandy aquifer. *Appl. Geochem.* 27 (12), 2435–2452.
- Baker, J.F., Fritz, P., 1981. Carbon isotope fractionation during microbial methane oxidation. *Nature* 293 (5830), 289–291.
- Becker, R.H., Clayton, R.N., 1972. Carbon isotopic evidence for the origin of a banded iron-formation in Western Australia. *Geochim. Cosmochim. Acta* 36 (5), 577–595.
- Berner, R.A., Morse, J.W., 1974. Dissolution kinetics of calcium carbonate in sea water: IV. Theory of calcite dissolution. *Am. J. Sci.* 274 (2), 108–134.
- Beutelspacher, H., Van der Marel, H.W., 1968. *Atlas of Electron Microscopy of Clay Minerals and Their Admixtures*. Elsevier, Amsterdam (333 pp).
- Bish, D.L., Post, J.E., 1993. Quantitative mineralogical analysis using the Rietveld full-pattern fitting method. *Am. Mineral.* 78 (9–10), 932–940.
- Boogs, S., 2009. *Petrology of Sedimentary Rocks*. Second edition. Cambridge University Press, Edinburgh (600 pp).
- Boulard, E., Guyot, F., Fiquet, G., 2012. The influence on Fe content on Raman spectra and unit cell parameters of magnesite–siderite solid solutions. *Phys. Chem. Miner.* 39 (3), 239–246.
- Budai, J.M., Martini, A.M., Walter, L.M., Ku, T.C.W., 2002. Fracture-fill calcite as a record of microbial methanogenesis and fluid migration: a case study from the Devonian Antrim Shale, Michigan Basin. *Geofluids* 2 (3), 163–183.
- Busenberg, E., Plummer, N., 1982. The kinetics of dissolution of dolomite in CO_2 - H_2O systems at 15 to 65 °C and 0 to 1 atm pCO_2 . *Am. J. Sci.* 282 (1), 45–78.
- Carothers, W.W., Adami, L.H., Rosenbauer, R.J., 1988. Experimental oxygen isotope fractionation between siderite-water and phosphoric acid liberated CO_2 -siderite. *Geochim. Cosmochim. Acta* 52 (10), 2445–2450.
- Chester, R., Hughes, M.J., 1967. A chemical technique for the separation of ferro-manganese minerals, carbonate minerals and adsorbed trace elements from pelagic sediments. *Chem. Geol.* 2, 249–262.
- Chou, L., Garrels, R.M., Wollast, R., 1989. Comparative study of the kinetics and mechanisms of dissolution of carbonate minerals. *Chem. Geol.* 78 (3–4), 269–282.
- Claff, S.R., Sullivan, L.A., Burton, E.D., Bush, R.T., 2010. A sequential extraction procedure for acid sulfate soils: partitioning of iron. *Geoderma* 155 (3–4), 224–230.
- Clayton, R.N., Jones, B.F., Berner, R.A., 1968. Isotope studies of dolomite formation under sedimentary conditions. *Geochim. Cosmochim. Acta* 32 (4), 415–432.
- Craddock, P.R., Dauphas, N., 2011. Iron and carbon isotope evidence for microbial iron respiration throughout the Archean. *Earth Planet. Sci. Lett.* 303 (1–2), 121–132.
- Craig, H., 1953. The geochemistry of the stable carbon isotopes. *Geochim. Cosmochim. Acta* 3 (2), 53–92.
- Curtis, C.D., Pearson, M.J., Somogyi, V.A., 1975. Mineralogy, chemistry, and origin of a concretionary siderite sheet (clay-ironstone band) in the Westphalian of Yorkshire. *Mineral. Mag.* 40 (312), 385–393.
- Curtis, C.D., Coleman, M.L., Love, L.G., 1986. Pore water evolution during sediment burial from isotopic and mineral chemistry of calcite, dolomite and siderite concretions. *Geochim. Cosmochim. Acta* 50 (10), 2321–2334.
- Das, S., Hendry, M.J., 2011. Application of Raman spectroscopy to identify iron minerals commonly found in mine wastes. *Chem. Geol.* 290 (3–4), 101–108.
- Degens, E.T., Epstein, S., 1964. Oxygen and carbon isotope ratios in coexisting calcites and dolomites from recent and ancient sediments. *Geochim. Cosmochim. Acta* 28 (1), 23–44.
- Dell'Abate, M.T., Benedetti, A., Brookes, P.C., 2003. Hyphenated techniques of thermal analysis for characterization of soil humic substances. *J. Sep. Sci.* 26 (5), 433–440.
- Drake, H., Åström, M.E., Heim, C., Åström, J., Whitehouse, M., Ivarsson, M., Siljeström, S., Sjövall, P., 2015. Extreme ^{13}C depletion of carbonates formed during oxidation of biogenic methane in fractured granite. *Nat. Commun.* 6, 7020.
- Duckworth, O.W., Martin, S.T., 2004a. Role of molecular oxygen in the dissolution of siderite and rhodochrosite. *Geochim. Cosmochim. Acta* 68 (3), 607–621.
- Duckworth, O.W., Martin, S.T., 2004b. Dissolution rates and pit morphologies of rhombohedral carbonate minerals. *Am. Mineral.* 89 (4), 554–563.
- Egger, M., Jilbert, T., Behrends, T., Rivard, C., Slomp, C.P., 2015. Vivianite is a major sink for phosphorus in methanogenic coastal surface sediments. *Geochim. Cosmochim. Acta* 169, 217–235.
- Fernández, A., Tang, J., Rosenheim, B.E., 2014. Siderite 'clumped' isotope thermometry: a new paleoclimate proxy for humid continental environments. *Geochim. Cosmochim. Acta* 126, 411–421.
- Fisher, Q., Raiswell, R., Marshall, J., 1998. Siderite concretions from nonmarine shales (Westphalian A) of the Pennines, England; controls on their growth and composition. *J. Sediment. Res.* 68 (5), 1034–1045.
- Gautelir, M., Oelkers, E.H., Schott, J., 1999. An experimental study of dolomite dissolution rates as a function of pH from -0.5 to 5 and temperature from 25 to 80 °C. *Chem. Geol.* 157 (1–2), 13–26.
- Gautier, D.L., 1982. Siderite concretions: indicators of early diagenesis in the Gammon Shale (Cretaceous). *J. Sediment. Res.* 52 (3), 859–871.
- Golubev, S.V., Bénéth, P., Schott, J., Dandurand, J.L., Castillo, A., 2009. Siderite dissolution kinetics in acidic aqueous solutions from 25 to 100 °C and 0 to 50 atm pCO_2 . *Chem. Geol.* 265 (1–2), 13–19.
- Griffioen, J., Vermooten, S., Janssen, G., 2013. Geochemical and palaeohydrological controls on the composition of shallow groundwater in the Netherlands. *Appl. Geochem.* 39, 129–149.
- Griffioen, J., Klaver, G., Westerhoff, W.E., 2016. The mineralogy of suspended matter, fresh and Cenozoic sediments in the Rhine-Meuse-Scheldt-Ems area, the Netherlands: an overview and review. *Neth. J. Geosci.* 95 (1), 23–107.
- Guo, H., Stüben, D., Berner, Z., 2007. Removal of arsenic from aqueous solution by natural siderite and hematite. *Appl. Geochem.* 22 (5), 1039–1051.
- Haese, R.R., Wallmann, K., Dahmke, A., Kretzmann, U., Müller, P.J., Schulz, H.D., 1997. Iron species determination to investigate early diagenetic reactivity in marine sediments. *Geochim. Cosmochim. Acta* 61 (1), 63–72.
- Hartog, N., Griffioen, J., van der Weijden, C.H., 2002. Distribution and reactivity of O_2 -reducing components in sediments from a layered aquifer. *Environ. Sci. Technol.* 36 (11), 2338–2344.
- Hartog, N., Griffioen, J., Van Bergen, P.F., 2005. Depositional and paleohydrogeological controls on the distribution of organic matter and other reactive reductants in aquifer sediments. *Chem. Geol.* 216 (1–2), 113–131.
- Hill, R.J., Howard, C.J., 1987. Quantitative phase analysis from neutron powder diffraction data using the Rietveld method. *J. Appl. Crystallogr.* 20 (6), 467–474.
- Huggett, J.M., Gale, A.S., McCarty, D., 2010. Petrology and palaeoenvironmental significance of authigenic iron-rich clays, carbonates and apatite in the Claiborne Group, Middle Eocene, NE Texas. *Sediment. Geol.* 228 (3), 119–139.
- Huisman, D.J., 1998. Geochemical characterization of subsurface sediments in the Netherlands. PhD Thesis (Wageningen, The Netherlands. 175 pp).
- Huisman, D.J., Klaver, G.T., Veldkamp, A., Van Os, B.J.H., 2000. Geochemical compositional changes at the Pliocene-Pleistocene transition in fluvio-deltaic deposits in the Tegel-Reuver area, Southeastern Netherlands. *Int. J. Earth Sci.* 89 (1), 154–169.
- Ithurbe, A., Peulon, S., Miserque, F., Beaucaire, C., Chaussé, A., 2009. Interaction between uranium (VI) and siderite (FeCO_3) surfaces in carbonate solutions. *Radiochim. Acta* 97 (3), 177–180.
- Ithurbe, A., Peulon, S., Miserque, F., Beaucaire, C., Chaussé, A., 2010. Retention and redox behavior of uranium (VI) by siderite (FeCO_3). *Radiochim. Acta* 98 (9–11), 563–568.
- Johnson, J.W., Nitao, J.J., Knauss, K.G., 2004. Reactive transport modelling of CO_2 storage in saline aquifers to elucidate fundamental processes, trapping mechanisms and sequestration partitioning. In: Baines, S.J., Worden, R.H. (Eds.), *Geological Storage of Carbon Dioxide* 233. Geological Society, London, Special Publications, pp. 107–128.
- Jönsson, J., Sherman, D.M., 2008. Sorption of As (III) and As (V) to siderite, green rust (fougerite) and magnetite: Implications for arsenic release in anoxic groundwaters. *Chem. Geol.* 255 (1–2), 173–181.
- König, I., Hollatz, R., 1990. A fingerprint technique using Mössbauer spectroscopy. *Hyperfine Interact.* 57 (1–4), 2245–2250.
- Kulp, J.L., Kent, P., Kerr, P.F., 1951. Thermal study of the Ca-Mg-Fe carbonate minerals. *Am. Mineral.* 36 (9–10), 643–670.
- Lal, R., 2008. Sequestration of atmospheric CO_2 in global carbon pools. *Energy Environ. Sci.* 1, 86–100.
- Lund, K., Fogler, H.S., McCune, C.C., 1973. Acidization I: the dissolution of dolomite in hydrochloric acid. *Chem. Eng. Sci.* 28 (3), 691–700.
- Lüttge, A., Winkler, U., Lasaga, A.C., 2003. Interferometric study of the dolomite dissolution: a new conceptual model for mineral dissolution. *Geochim. Cosmochim. Acta* 67 (6), 1099–1116.
- Matsumoto, R., 1989. Isotopically heavy oxygen-containing siderite derived from the decomposition of methane hydrate. *Geology* 17 (8), 707–710.
- McCrea, J.M., 1950. On the isotopic chemistry of carbonates and a paleotemperature scale. *J. Chem. Phys.* 18 (6), 849–857.
- Meyers, P.A., 1994. Preservation of elemental and isotopic source identification of sedimentary organic matter. *Chem. Geol.* 114 (3), 289–302.
- Morse, J.W., Arvidson, R.S., 2002. The dissolution kinetics of major sedimentary carbonate minerals. *Earth Sci. Rev.* 58 (1–2), 51–84.
- Mortimer, R.J.G., Coleman, M.L., 1997. Microbial influence on the oxygen isotopic composition of diagenetic siderite. *Geochim. Cosmochim. Acta* 61 (8), 1705–1711.
- Mortimer, R.J.G., Galsworthy, A.M.J., Bottrell, S.H., Wilmot, L.E., Newton, R.J., 2011. Experimental evidence for rapid biotic and abiotic reduction of Fe (III) at low temperatures in salt marsh sediments: a possible mechanism for formation of modern sedimentary siderite concretions. *Sedimentology* 58 (6), 1514–1529.
- Mozley, P.S., 1989. Relation between depositional environment and the elemental composition of early diagenetic siderite. *Geology* 17 (8), 704–706.
- Mozley, P.S., Carothers, W.W., 1992. Elemental and isotopic composition of siderite in the Kuparuk Formation, Alaska: effect of microbial activity and water/sediment interaction on early pore-water. *J. Sediment. Res.* 62 (4), 681–692.
- Mozley, P.S., Wersin, P., 1992. Isotopic composition of siderite as an indicator of depositional environment. *Geology* 20 (9), 817–820.
- Pearson, M.J., 1974. Sideritic concretions from the Westphalian of Yorkshire: a chemical investigation of the carbonate phase. *Mineral. Mag.* 39 (306), 696–699.
- Pecharsky, V., Zavalij, P., 2009. *Fundamentals of Powder Diffraction and Structural Characterization of Materials*. Second edition. Springer, New York (741 pp).
- Plummer, L.N., Wigley, T.M.L., Parkhurst, D.L., 1978. The kinetics of calcite dissolution in CO_2 -water systems at 5 ° to 60 °C and 0.0 to 1.0 atm CO_2 . *Am. J. Sci.* 278 (2), 179–216.
- Pokrovsky, O.S., Golubev, S.V., Schott, J., Castillo, A., 2009. Calcite, dolomite and magnesite dissolution kinetics in aqueous solutions at acid to circumneutral pH, 25 to 150 °C and 1 to 55 atm pCO_2 : new constraints on CO_2 sequestration in sedimentary basins. *Chem. Geol.* 265 (1–2), 20–32.

- Postma, D., 1977. The occurrence and chemical composition of recent Fe-rich mixed carbonates in a river bog. *J. Sediment. Petrol.* 47 (3), 1089–1098.
- Postma, D., 1981. Formation of siderite and vivianite and the pore-water composition of a recent bog sediment in Denmark. *Chem. Geol.* 31, 225–244.
- Postma, D., 1982. Pyrite and siderite formation in brackish and freshwater swamp sediments. *Am. J. Sci.* 282 (8), 1151–1183.
- Poulton, S.W., Canfield, D.E., 2005. Development of a sequential extraction procedure for iron: implications for iron partitioning in continentally derived particulates. *Chem. Geol.* 214 (3–4), 209–221.
- Pye, K., Dickson, J., Schiavon, N., Coleman, M.L., Cox, M., 1990. Formation of siderite-Mg-calcite-iron sulphide concretions in intertidal marsh and sandflat sediments, north Norfolk, England. *Sedimentology* 37 (2), 325–343.
- Rickard, D.T., Sjöberg, E.L., 1983. Mixed kinetic control of calcite dissolution rates. *Am. J. Sci.* 283 (8), 815–830.
- Rochelle, C.A., Czernichowski-Lauriol, I., Milodowski, A.E., 2004. The impact of chemical reactions on CO₂ storage in geological formations: a brief review. In: Baines, S.J., Worden, R.H. (Eds.), *Geological Storage of Carbon Dioxide 233*. Geol. Soc. Lond., Spec. Publ., pp. 87–106.
- Rosenbaum, J., Sheppard, S.M.F., 1986. An isotopic study of siderites, dolomites and ankerites at high temperatures. *Geochim. Cosmochim. Acta* 50 (6), 1147–1150.
- Rudnick, R.L., Gao, S., 2003. Composition of the continental crust. In: Rudnick, R.L. (Ed.), *The Crust II: Holland, H.D., Turekian, K.K. (Eds.), 3. Treatise on Geochemistry*. Amsterdam: Elsevier, pp. 1–64.
- Rossi, C., Marfil, R., Ramseyer, K., Permanyer, A., 2001. Facies-related diagenesis and multiphase siderite cementation and dissolution in the reservoir sandstones of the Khatatba Formation, Egypt's Western Desert. *J. Sediment. Res.* 71 (3), 459–472.
- Sackett, W.M., 1964. The depositional history and isotopic organic carbon composition of marine sediments. *Mar. Geol.* 2 (3), 173–185.
- Sapota, T., Aldahan, A., Al-Aasm, I.S., 2006. Sedimentary facies and climate control on formation of vivianite and siderite microconcretions in sediments of Lake Baikal, Siberia. *J. Paleolimnol.* 36 (3), 245–257.
- Saunders, J.A., Swann, C.T., 1992. Nature and origin of authigenic rhodochrosite and siderite from the Paleozoic aquifer, northeast Mississippi, U.S.A. *Appl. Geochem.* 7 (4), 375–387.
- Scheinost, A.C., Charlet, L., 2008. Selenite reduction by mackinawite, magnetite and siderite: XAS characterization of nanosized redox products. *Environ. Sci. Technol.* 42 (6), 1984–1989.
- Sitko, R., Zawisza, B., Krzykowski, T., Malicka, E., 2009. Determination of chemical composition of siderite in concretions by wavelength-dispersive X-ray spectrometry following selective dissolution. *Talanta* 77 (3), 1105–1110.
- Sjöberg, E.L., Rickard, D.T., 1984a. Calcite dissolution kinetics: surface speciation and the origin of the variable pH dependence. *Chem. Geol.* 42 (1–4), 119–136.
- Sjöberg, E.L., Rickard, D.T., 1984b. Temperature dependence of calcite dissolution kinetics between 1 and 62 °C at pH 2.7 to 8.4 in aqueous solutions. *Geochim. Cosmochim. Acta* 48 (3), 485–493.
- Smykatz-Kloss, W., 1982. Application of differential thermal analysis in mineralogy. *J. Therm. Anal.* 23 (1), 15–44.
- Soukup, D.A., Vegas, L., Buck, B.J., Harris, W., 2008. Preparing soils for mineralogical analyses. In: Ulery, A.L., Drees, L.R. (Eds.), *Methods of Soil Analysis Part 5-Mineralogical Methods*. Madison, Soil Science Society of America, pp. 13–31.
- Spadini, L., Bott, M., Wehrli, B., Manceau, A., 2003. Analysis of the major Fe bearing mineral phases in recent lake sediments by EXAFS spectroscopy. *Aquat. Geochem.* 9 (1), 1–17.
- Spötl, C., Vennemann, T.W., 2003. Continuous-flow IRMS analysis of carbonate minerals. *Rapid Commun. Mass Spectrom.* 17 (9), 1004–1006.
- Sternbeck, J., Sohlenius, G., 1997. Authigenic sulfide and carbonate mineral formation in Holocene sediments of the Baltic Sea. *Chem. Geol.* 135 (1–2), 55–73.
- Stumm, W., Morgan, J.J., 1996. *Aquatic Chemistry: Chemical Equilibria and Rates in Natural Waters*. Third edition. John Wiley & Sons, New York (1040 pp).
- Swart, P.K., Melim, L.A., 2000. The origin of dolomites in Tertiary sediments from the margin of Great Bahama Bank. *J. Sediment. Res.* 70 (3), 738–748.
- Tessier, A., Campbell, P.G.C., Bisson, M., 1979. Sequential extraction procedure for the speciation of particulate trace metals. *Anal. Chem.* 51 (7), 844–851.
- Van Cappellen, P., Charlet, L., Stumm, W., Wersin, P., 1993. A surface complexation model of the carbonate mineral-aqueous solution interface. *Geochim. Cosmochim. Acta* 57 (15), 3505–3518.
- Van der Marel, H.W., Beutelspacher, H., 1976. *Atlas of Infrared Spectroscopy of Clay Minerals and Their Admixtures*. Elsevier Publishing Company, Amsterdam (396 pp).
- Vriens, B.P.J.M., 2011. The diagenetic origin of siderite in Early Pleistocene fluviodeltaic deposits in Maalbeek, The Netherlands. MSc Thesis. Utrecht University, the Netherlands (49 pp).
- Walters, L.J., Claypool, G.E., Choquette, P.W., 1972. Reaction rates and $\delta^{18}\text{O}$ variation for the carbonate-phosphoric acid preparation method. *Geochim. Cosmochim. Acta* 36 (2), 129–140.
- Ward, C.R., Gómez-Fernández, F., 2003. Quantitative mineralogical analysis of Spanish roofing slates using the Rietveld method and X-ray powder diffraction data. *Eur. J. Mineral.* 15 (6), 1051–1062.
- Warne, S.S.J., Morgan, D.J., Milodowski, A.E., 1981. Thermal analysis studies of the dolomite, ferroan dolomite, ankerite series. Part 1. Iron content recognition and determination by variable atmosphere DTA. *Thermochim. Acta* 51 (2–3), 105–111.
- Weidler, P.G., Luster, J., Schneider, J., Sticher, H., Gehring, A.U., 1998. The Rietveld method applied to the quantitative mineralogical and chemical analysis of a ferrallitic soil. *Eur. J. Soil Sci.* 49 (1), 95–105.
- Wilkinson, M., Haszeldine, R.S., Fallick, A.E., Osborne, M.J., 2000. Siderite zonation within the Brent Group: microbial influence or aquifer flow? *Clay Miner.* 35 (1), 107.
- Whiticar, M.J., 1999. Carbon and hydrogen isotope systematics of bacterial formation and oxidation of methane. *Chem. Geol.* 161 (1–3), 291–314.
- Wollast, R., 1990. Rate and mechanism of dissolution of carbonates in the system CaCO₃–MgCO₃. In: Stumm, W. (Ed.), *Aquatic Chemical Kinetics*. John Wiley & Sons, New York, pp. 431–445.